Journal of Organometallic Chemistry, 263 (1984) 75–92
Elsevier Sequoia S.A., Lausanne – Printed in The Netherlands

RELATIVE RATES OF LIGAND SUBSTITUTION ON NONACARBONYLTRIS(μ-HYDRIDO)(μ_3-METHYLIDYNE)TRIRUTHENIUM CLUSTERS. THE CRYSTAL STRUCTURE OF $(\mu\text{-H})_3Ru_3(\mu_3\text{-CPh})(CO)_7(AsPh_3)_2$

ZURAIDAH ABDUL RAHMAN, LAWRENCE R. BEANAN, LYNN M. BAVARO, SANDEEP P. MODI, JEROME B. KEISTER *, and MELVYN ROWEN CHURCHILL *

Department of Chemistry, State University of New York at Buffalo, Buffalo, New York 14214 (U.S.A.)

(Received July 26th, 1983)

Summary

Substitution on $(\mu\text{-H})_3Ru_3(\mu_3\text{-CX})(CO)_9$ (X = OMe, Me, Cl, Ph) by triphenylarsine proceeds sequentially to $(\mu\text{-H})_3Ru_3(\mu_3\text{-CX})(CO)_{9-n}(AsPh_3)_n$ ($n = 1, 2, 3$). A single-crystal X-ray crystallographic study of $(\mu\text{-H})_3Ru_3(\mu_3\text{-CPh})(CO)_7(AsPh_3)_2$ has been performed. This complex crystallizes in the centrosymmetric monoclinic space group $C2/c$ [No. 15] with a 36.746(19), b 12.743(6), c 22.802(11) Å, β 108.60(4)°, V 10119 Å^3 and $Z = 8$. Data for 2θ 4.0–35.0° (Mo-K_α) were collected on a Syntex $P2_1$ automated four-circle diffractometer and the structure was refined to R_F 7.2% for all 3208 reflections (R_F 5.4% for those 2523 reflections with $|F_o| > 6\sigma(|F_o|)$). The crystal structure establishes axial coordination for the triphenylarsine ligands on different metal atoms. The rate of CO dissociation from $(\mu\text{-H})_3Ru_3(\mu_3\text{-CX})(CO)_9$ is found to depend upon X in the order: X = OMe (36) ≫ Me (3.2) > Cl (2.3) > Ph (1) at 298 K. The labilizing effect of the methoxy substituent is attributed to stabilization of the transition state by π-donation to the Ru_3C core.

Introduction

Systematic studies of reactivity are necessary for proper definition of the unique features of the chemistry of metal carbonyl clusters. Two cluster series which are especially suitable candidates for such studies are the $Co_3(\mu_3\text{-CX})(CO)_9$ clusters [1], which have been extensively examined for over 20 years, and the analogous $(\mu\text{-H})_3M_3(\mu_3\text{-CX})(CO)_9$ (M = Ru or Os) [2–5] series, where X = H, alkyl, aryl, halide, carbomethoxy and others. We have undertaken investigations of the methylidynetriruthenium clusters with the goals of (1) comparing and contrasting the chemical, physical and structural properties of these related cluster series and (2) determining the reactivity of the hydride ligands, particularly as influenced by the methylidyne substituent and other ligands on the Ru_3C core. We have previously

0022-328X/84/$03.00

described reactions of $(\mu\text{-H})_3Ru_3(\mu_3\text{-CX})(CO)_9$ with alkenes [6] and alkynes [7] involving hydrogen transfer and have investigated the mechanism of reversible reductive elimination of molecular hydrogen from $(\mu\text{-H})_3Ru_3(\mu_3\text{-COMe})(CO)_9$ [8]. The chemistry of these methylidyne clusters of the iron triad is proving even richer than that of the cobalt analogs.

The rate-determining step in many reactions of saturated clusters such as $Co_3(\mu_3\text{-CX})(CO)_9$ and $(\mu\text{-H})_3Ru_3(\mu_3\text{-CX})(CO)_9$ is ligand dissociation to generate an unsaturated and reactive intermediate [9]. Thus, an understanding of reactivity in these systems requires information about the rates and mechanisms of carbonyl substitutions, particularly the relative rates as a function of the nature of X. Two studies of ligand substitution on $Co_3(\mu_3\text{-CX})(CO)_9$ have been reported [10,11]. We describe here a study of the kinetics of substitution on $(\mu\text{-H})_3Ru_3(\mu_3\text{-CX})(CO)_9$ (X = OMe, Me, Cl, Ph) by triphenylarsine and the characterization of the products $(\mu\text{-H})_3Ru_3(\mu_3\text{-CX})(CO)_{9-n}(AsPh_3)_n$ ($n = 1, 2, 3$), including an X-ray crystallographic determination of the structure of $(\mu\text{-H})_3Ru_3(\mu_3\text{-CPh})(CO)_7(AsPh_3)_2$. These results lead to a re-interpretation of the influence of the methylidyne substituent upon the rate of carbonyl substitution in both the methylidyne-tricobalt and -triruthenium systems and establish the differing coordination geometries for the two series.

Experimental

The clusters $(\mu\text{-H})_3Ru_3(\mu_3\text{-CX})(CO)_9$ (X = Cl [2], Ph [2], H [2], CO_2Me [2], OMe [3] and Me [4]) and $Co_3(\mu\text{-CX})(CO)_9$ (X = Cl [12a] and OMe [12b]) were prepared according to literature procedures. Triphenylarsine was purchased from Alfa and was used as received.

Proton NMR spectra were recorded on a Varian EM-390 instrument. Infrared spectra were obtained on a Perkin–Elmer 467 spectrophotometer and were calibrated against cyclohexane. Mass spectra were recorded at the Penn State University Mass Spectrometry Laboratory. Elemental analyses were performed by Schwarzkopf Laboratory.

The substituted derivatives $(\mu\text{-H})_3Ru_3(\mu_3\text{-CX})(CO)_{9-n}L_n$ were prepared by mixing the parent carbonyl with a 1 to 10 molar excess of ligand L in cyclohexane or 1,2-dichloroethane and then monitoring the reaction until the desired product predominated. The products were separated by thin layer chromatography and were recrystallized after extraction. Typical examples are as follows.

$(\mu\text{-H})_3Ru_3(\mu_3\text{-CPh})(CO)_8(AsPh_3)$. A solution of $(\mu\text{-H})_3Ru_3(\mu_3\text{-CPh})(CO)_9$ (114 mg, 0.117 mmol) and triphenylarsine (50 mg, 0.16 mmol) in heptane (50 ml) was heated at 35°C under nitrogen with stirring for 7 h. After stirring overnight at room temperature, the solution was evaporated to dryness. The products were then separated by thin layer chromatography on silica gel, eluting with 3/1 hexane/dichloromethane. Extraction of the second yellow band with dichloromethane and evaporation yielded yellow crystals (104 mg, 64%).

Anal. Found: C, 42.58; H, 2.56. $AsC_{33}H_{23}O_8Ru_3$ calcd.: C, 42.82; H, 2.50%. Mass spectrum, m/e 928 ($^{102}Ru_3$).

$(\mu\text{-H})_3Ru_3(\mu_3\text{-CPh})(CO)_7(AsPh_3)_2$. A solution of $(\mu\text{-H})_3Ru_3(\mu_3\text{-CPh})(CO)_8(AsPh_3)$ (70 mg, 0.076 mmol), $(\mu\text{-H})_3Ru_3(\mu_3\text{-CPh})(CO)_9$ (55 mg, 0.085 mmol) and triphenylarsine (174 mg, 0.567 mmol) in heptane (50 ml) was heated under nitrogen for 8 h at 35–40°C. Then the solution was evaporated to dryness and the

TABLE 1

INFRARED SPECTRAL DATA FOR $(\mu\text{-H})_3Ru_3(\mu_3\text{-CX})(CO)_{9-n}L_n$ TAKEN BETWEEN 2150 AND 1700 cm^{-1} IN CYCLOHEXANE SOLUTION

X	L	n	
Ph	$AsPh_3$	1	2093(m), 2074(s), 2033(s), 2025(m), 2008(w), 1990(vw), 1973(w)
Ph	$AsPh_3$	2	2092(vw), 2079(s), 2074(sh), 2032(vs), 2024(vs) 2011(m), 2004(w), 1976(s)
Ph	$AsPh_3$	3	2040(s), 2018(s), 1970(s)
Ph	PPh_3	3	2040(s), 2020(vs), 1974(s)
Ph	$P(OMe)_3$	3	2046(m), 2022(vs), 1973(s)
Cl	$AsPh_3$	2	2084(s), 2043(vs), 2036(vs), 2020(m), 2016(s), 1990(m)
Cl	$AsPh_3$	3	2085(w), 2046(s), 2025(vs), 1973(s)
Me	$AsPh_3$	3	2076(vw), 2037(s), 2012(s), 1963(m)
OMe	$AsPh_3$	3	2038(s), 2012(s) 1964(s)
OMe	$SbPh_3$	3	2040(s), 2014(s), 1966(s)
OMe	$SbPh_3$ [a]	2	2084(m), 2076(m), 2037(s), 2025(s), 2015(s), 1999(w), 1963(s), 1958(m), 1947(w)
OMe	PPh_3 [b]	3	2062(w), 2038(s), 2013(vs), 1963(s)

[a] Contaminated with $(\mu\text{-H})_3Ru_3(\mu_3\text{-COMe})(CO)_6(SbPh_3)$. [b] In dichloromethane.

TABLE 2

^1H NMR DATA [a] FOR $(\mu\text{-H})_3Ru_3(\mu_3\text{-CX})(CO)_{9-n}L_n$

X	L	n	hydride resonances (τ)
Ph	$AsPh_3$	0	27.30 (s,3H)
Ph	$AsPh_3$	1	27.16(t,1H), 26.54(d,2H), J 3Hz
Ph	$AsPh_3$	2	26.22(d,2H), 25.44(t,1H), J 3Hz
Ph	$AsPh_3$	3	24.74(s,3H)
Cl	$AsPh_3$	0	27.46(s,3H)
Cl	$AsPh_3$	1	27.35(t,1H), 26.70(d,2H), J 3 Hz
Cl	$AsPh_3$	2	26.34(d,2H), 25.68(t,1H), J 3 Hz
Cl	$AsPh_3$	3	25.12(s,3H)
Me	$AsPh_3$	0	27.38(s,3H)
Me	$AsPh_3$	1	27.25(t,1H), 26.64(d,2H), J 3 Hz
Me	$AsPh_3$	2	26.24(d,2H), 25.56(t,1H), J 3 Hz
Me	$AsPh_3$	3	24.96(s,3H)
OMe	$AsPh_3$	0	28.64(s,3H)
OMe	$AsPh_3$	1	28.56(t,1H), 27.94(d,2H), J 3 Hz
OMe	$AsPh_3$	2	27.50(d,2H), 26.92(t,1H), J 3 Hz
OMe	$AsPh_3$	3	26.34(s,3H)
OMe	$SbPh_3$	1 [b,c]	27.58(t,1H), 26.91(d,2H), J 3 Hz
OMe	$SbPh_3$	2 [b,d]	26.74(d,2H), 26.15(t,1H), J 3 Hz
OMe	$SbPh_3$	3 [b,e]	25.78(s,3H)
Ph	PPh_3	3	25.2(t,3H), J(P–H) 7.2 Hz
OMe	PPh_3	3 [f]	25.1(t,3H), J(P–H) 8.1 Hz
Ph	$P(OMe)_3$	3	26.6(t,3H), J(P–H) 8.1 Hz

[a] In 1,2-dichloroethane, unless specified. [b] In deuteriochloroform. [c] Other signals: 2.9(m 15H), 6.09(s,3H). [d] Other signals: 2.9(m,30H), 5.91(s,3H). [e] Other signals: 2.9(m,45H), 5.78(s,3H). [f] Other signals: 2.9(m,45H), 6.02(s,3H).

product mixture was separated by thin layer chromatography on silica gel, eluting with 3/1 hexane/dichloromethane. Extraction of the second yellow band with dichloromethane and evaporation of the solution to dryness yielded the product (99 mg, 40%). The product was recrystallized from acetone.

$(\mu$-H)$_3$Ru$_3(\mu_3$-CPh)(CO)$_6$(AsPh$_3$)$_3$. A solution of $(\mu$-H)$_3$Ru$_3(\mu_3$-CPh)-(CO)$_8$(AsPh$_3$) (34 mg, 0.037 mmol), $(\mu$-H)$_3$Ru$_3(\mu_3$-CPh)(CO)$_7$(AsPh$_3$)$_2$ (99 mg, 0.082 mmol) and triphenylarsine (146 mg, 0.48 mmol) in 1,2-dichloroethane (50 ml) was heated at 40°C for 7 h under nitrogen. Separation of the product mixture was achieved by thin layer chromatography on silica gel, eluting with 1/1 hexane/dichloromethane. Extraction of the second yellow band with dichloromethane and evaporation of the solution to dryness yielded the product as yellow crystals (55 mg, 20%). The product was recrystallized from acetone for analysis.

Anal. Found: C, 54.17; H, 3.79; As, 15.53; Ru, 20.15. $As_3C_{67}H_{53}O_6Ru_3$ calcd.: C, 54.29; H, 3.60; As, 15.16; Ru, 20.45%.

$(\mu$-H)$_3$Ru$_3(\mu_3$-COMe)(CO)$_7$(AsPh$_3$)$_2$. A solution of $(\mu$-H)$_3$Ru$_3(\mu_3$-COMe)(CO)$_9$ (107 mg, 0.178 mmol) and triphenylarsine (109 mg, 0.357 mmol) in cyclohexane (25 ml) was stirred under nitrogen for 12 h at room temperature. The product mixture was separated by thin layer chromatography on silica gel, eluting with dichloromethane/cyclohexane (1/1), to give three yellow bands. Extraction of the third band with dichloromethane and evaporation of the solution to dryness yielded $(\mu$-H)$_3$Ru$_3(\mu_3$-COMe)(CO)$_7$ (AsPh$_3$)$_2$ (196 mg, 95%). The product was recrystallized from dichloromethane/methanol at −16°C to give 50 mg.

Anal. Found: C, 46.78; H, 3.35; As, 13.19; Ru, 25.87. $As_2C_{45}H_{36}O_8Ru_3$ calcd.: C, 46.68; H, 3.13; As, 12.94; Ru, 26.19%.

Co$_3(\mu_3$-COMe)(CO)$_8$(PPh$_3$). A solution of Co$_3(\mu_3$-COMe)(CO)$_9$ (107 mg, 0.227 mmol) and triphenylphosphine (158 mg, 0.603 mmol) in cyclohexane (50 ml) was stirred overnight under nitrogen. The solvent was removed on a rotary evaporator and the residue was purified by thin layer chromatography on silica gel, eluting with 1/9 dichloromethane/cyclohexane. The second purple-black band was extracted with dichloromethane and was characterized spectroscopically as Co$_3(\mu_3$-COMe)(CO)$_8$(PPh$_3$). Yield 62 mg, 39%.

IR(C_6H_{12}): 2076(m), 2032(vs), 2012(s), 1996(w), 1984(vw), 1975(vw) cm^{-1}. ^1H NMR ($CDCl_3$): τ 2.6 (m, 15 H), 6.17 (s, 3 H).

Kinetics of substitution on $(\mu$-H)$_3$Ru$_3(\mu_3$-CX)(CO)$_9$. A solution of 25–30 mg of $(\mu$-H)$_3$Ru$_3(\mu_3$-CX)(CO)$_9$ and the desired amount of triphenylarsine was prepared in 0.60 ml of 1,2-dichloroethane in a capped 5 mm NMR tube. A NMR spectrum of the hydride region was recorded and then the tube was immersed in a Lauda constant temperature bath. At one to two hour intervals the tube was removed and the spectrum was recorded and integrated. Approximately 10 minutes was required for each measurement. The influence of the change in temperature during the sampling upon the rate was found to be negligible at 298 K to 308 K for X = Me, Cl or Ph. For X = OMe the rate was too fast to be measured in this manner, and in this case all measurements were made with the temperature of the NMR probe controlled to the desired value. Runs were terminated when precipitation of $(\mu$-H)$_3$Ru$_3(\mu_3$-CX)(CO)$_6$(AsPh$_3$)$_3$ was noted.

Rates were determined from plots of the mole fraction of each cluster species as a function of time. The integrals of all hydride resonances were taken and the mole fraction of each species was determined as the integral of the hydride signals for that

(Continued on p. 82)

TABLE 3

RATE CONSTANTS FOR SUBSTITUTION ON $(\mu\text{-H})_3Ru_3(\mu_3\text{-CX})(CO)_9$ BY TRIPHENYLARSINE

X [a]	$[AsPh_3]$(M)	T(K)	$k_1(\times 10^5\ s^{-1})$ [b]	$k_1(\times 10^5\ s^{-1})$ [c]	$k_2(\times 10^5\ s^{-1})$ [c]
Ph	0.76	298	1.7	1.8	1.4
Ph	0.77	303	4.1	4.6	2.9
Ph	1.53	303	3.7	4.4	2.9
Ph	0.85	308	6.4	6.2	4.3
Cl	0.82	298	3.9	3.9	2.6
Cl	1.66	298	3.9	3.8	2.8
Cl	1.67	303	8.9	8.6	5.5
Cl	0.82	308	14	11	6.8
Me	0.72	298	5.6	6.0	4.0
Me	1.70	298	5.3	4.8	3.5
Me	0.71	303	11.6	6.8	3.6
Me	1.70	303	10.5	9.2	7.7
Me	0.82	308	24	24	22
OMe	0.94	288	15	15	10
OMe	1.02	298	62	67	44
OMe	0.83	308	400	390	200

[a] Initial concentration of cluster ca. 0.08 M. [b] Determined by least-squares fit of ln(mole fraction of $(\mu\text{-H})_3Ru_3(\mu_3\text{-CX})(CO)_9$) vs. time. [c] Determined by computer fit of concentrations of all species as a function of time.

TABLE 4

X-RAY DIFFRACTION DATA FOR $(\mu\text{-H})_3Ru_3(\mu_3\text{-CPh})(CO)_7(AsPh_3)_2$

(A) Crystal parameters at 23°C	
Crystal system:	Monoclinic
Space group:	$C2/c$ [No. 15] [a]
a	36.746(19) Å
b	12.743(6) Å
c	22.802(11) Å
β	108.599(41)°
V	10119.4 Å^3
Z	8
mol. wt.	1203.9
ρ(calcd)	1.58 g cm^{-3}
μ(Mo-K_α)	22.8 cm^{-1}
(B) Measurement of data	
Diffractometer	Syntex $P2_1$
Radiation	Mo-K_α ($\bar{\lambda}$ 0.710730 Å)
Monochromator	highly oriented graphite, equatorial mode
Scan type	coupled θ(crystal)–2θ(counter)
Scan speed	3.0 deg/min
Reflections measured	$+h, +k, \pm l$ for $2\theta = 4.0$–$35.0°$
Number of independent reflections	3208
Standards	3 every 97 reflections; no significant variations observed

[a] Systematic absences were hkl for $h + k = 2n + 1$ and $h0l$ for $l = 2n$ ($h = 2n$) consistent with the non-centrosymmetric space group Cc [No. 9] or the centrosymmetric space group $C2/c$ [No. 15]; the latter was selected on the basis of (a) the number of molecules per unit cell; (b) intensity statistics, and (c) the successful solution of the structure in this higher symmetry space group.

TABLE 5

POSITIONAL PARAMETERS FOR $(\mu\text{-H})_3Ru_3(\mu_3\text{-CPh})(CO)_7(AsPh_3)_2$

Atom	x	y	z	B_{iso}	Atom	x	y	z	B_{iso}
Ru(1)	0.14273(5)	0.36716(13)	0.66452(8)		H(1)	0.1235(36)	0.498(10)	0.6461(58)	2.5
Ru(2)	0.13339(5)	0.56599(13)	0.71654(8)		H(2)	0.1716(40)	0.570(10)	0.7417(56)	2.5
Ru(3)	0.20851(5)	0.48126(14)	0.73627(8)		H(3)	0.1822(79)	0.441(21)	0.682(13)	2.5
As(1)	0.13644(6)	0.34804(17)	0.55190(10)		H(4)	0.2030	0.2709	0.8202	6.0
As(2)	0.11798(6)	0.73104(17)	0.65113(10)		H(5)	0.1961	0.1753	0.9039	6.0
O(1A)	0.17870(45)	0.1505(12)	0.69135(74)		H(6)	0.1447	0.2088	0.9459	6.0
O(1B)	0.06380(47)	0.2878(13)	0.66096(74)		H(7)	0.1014	0.3457	0.9029	6.0
O(2A)	0.15105(48)	0.6730(13)	0.83979(76)		H(8)	0.1082	0.4421	0.8171	6.0
O(2B)	0.05136(44)	0.5241(13)	0.71394(75)		H(9)	0.1595	0.2215	0.4569	6.0
O(3A)	0.25986(43)	0.2884(12)	0.76828(77)		H(10)	0.1439	0.0543	0.4136	6.0
O(3B)	0.26158(48)	0.5800(13)	0.66910(76)		H(11)	0.0996	−0.0471	0.4375	6.0
O(3C)	0.24314(46)	0.6002(13)	0.85656(75)		H(12)	0.0692	0.0049	0.5156	6.0
C(1B)	0.09376(69)	0.3167(17)	0.6603(10)	3.41(52)	H(13)	0.0906	0.1691	0.5656	6.0
C(1A)	0.16566(63)	0.2293(19)	0.6823(10)	3.27(52)	H(15)	0.0760	0.4969	0.5540	6.0
C(2A)	0.14484(64)	0.6321(18)	0.7914(12)	4.11(57)	H(16)	0.0223	0.5757	0.4776	6.0
C(2B)	0.08154(69)	0.5405(17)	0.7134(10)	3.27(52)	H(17)	0.0078	0.5392	0.3751	6.0
C(3A)	0.24122(66)	0.3606(19)	0.7595(10)	3.31(53)	H(18)	0.0473	0.4287	0.3390	6.0
C(3B)	0.24242(65)	0.5465(17)	0.6922(10)	3.34(54)	H(19)	0.1049	0.3531	0.4122	6.0
C(3C)	0.23063(67)	0.5527(19)	0.8130(12)	4.06(58)	H(21)	0.2138	0.2829	0.5983	6.0
C(1)	0.15877(53)	0.4262(25)	0.75418(85)	2.22(44)	H(22)	0.2743	0.3206	0.5814	6.0
C(2)	0.15655(55)	0.3685(15)	0.80781(88)	2.47(45)	H(23)	0.2735	0.4449	0.5015	6.0
C(3)	0.18200(61)	0.2885(17)	0.8363(10)	3.88(53)	H(24)	0.2173	0.5328	0.4434	6.0
C(4)	0.17740(66)	0.2314(18)	0.8862(11)	4.72(58)	H(25)	0.1572	0.4928	0.4659	6.0
C(5)	0.14737(64)	0.2513(17)	0.9115(10)	3.94(53)	H(27)	0.0635	0.9107	0.6411	6.0
C(6)	0.12216(62)	0.3287(17)	0.8864(10)	4.06(53)	H(28)	0.0655	1.0717	0.6985	6.0
C(7)	0.12671(66)	0.3853(18)	0.8354(11)	4.69(57)	H(29)	0.1184	1.1041	0.7823	6.0
C(8)	0.12824(59)	0.2097(16)	0.51732(95)	3.26(49)	H(30)	0.1678	0.9907	0.8164	6.0
C(9)	0.14220(62)	0.1760(18)	0.4709(10)	4.13(54)	H(31)	0.1679	0.8362	0.7611	6.0
C(10)	0.13234(69)	0.0801(20)	0.4450(11)	5.15(60)	H(33)	0.1699	0.6228	0.5942	6.0

C(11)	0.10657(76)	0.0200(21)	0.4597(12)	6.44(67)	H(34)	0.2155	0.6720	0.5482	6.0
C(12)	0.08833(70)	0.0492(19)	0.5046(11)	5.44(62)	H(35)	0.2292	0.8470	0.5435	6.0
C(13)	0.10128(62)	0.1445(17)	0.5339(10)	3.91(53)	H(36)	0.1981	0.9786	0.5727	6.0
C(14)	0.09415(57)	0.4160(16)	0.4894(10)	3.08(48)	H(37)	0.1523	0.9307	0.6214	6.0
C(15)	0.07087(61)	0.4826(17)	0.5099(10)	3.72(52)	H(39)	0.0355	0.6959	0.6330	6.0
C(16)	0.03901(64)	0.5281(17)	0.4645(11)	4.30(55)	H(40)	−0.0227	0.7366	0.5554	6.0
C(17)	0.03063(66)	0.5072(18)	0.4047(11)	4.76(58)	H(41)	−0.0194	0.7976	0.4560	6.0
C(18)	0.05416(68)	0.4416(19)	0.3840(11)	4.97(59)	H(42)	0.0383	0.8233	0.4371	6.0
C(19)	0.08730(64)	0.3964(17)	0.4263(11)	4.28(54)	H(43)	0.0952	0.7926	0.5175	6.0
C(20)	0.18156(57)	0.3856(16)	0.53299(93)	2.87(47)					
C(21)	0.21463(63)	0.3343(17)	0.5668(10)	3.79(52)					
C(22)	0.25053(70)	0.3556(19)	0.5572(11)	5.54(63)					
C(23)	0.24969(72)	0.4303(19)	0.5098(11)	5.19(59)					
C(24)	0.21651(74)	0.4821(19)	0.4756(12)	5.64(63)					
C(25)	0.18150(63)	0.4576(18)	0.4890(10)	4.41(56)					
C(26)	0.11688(63)	0.8603(17)	0.6967(10)	3.76(51)					
C(27)	0.08492(68)	0.9276(19)	0.6761(11)	5.02(59)					
C(28)	0.08611(79)	1.0228(22)	0.7104(13)	6.69(70)					
C(29)	0.11745(78)	1.0405(20)	0.7602(12)	5.85(64)					
C(30)	0.14698(70)	0.9750(19)	0.7803(11)	5.03(59)					
C(31)	0.14683(60)	0.8833(17)	0.7476(10)	3.48(50)					
C(32)	0.15677(59)	0.7735(17)	0.6100(10)	3.51(50)					
C(33)	0.17556(62)	0.6947(17)	0.5899(10)	3.53(50)					
C(34)	0.20224(68)	0.7231(19)	0.5639(11)	5.14(60)					
C(35)	0.20959(66)	0.8290(20)	0.5605(11)	4.81(58)					
C(36)	0.19240(68)	0.9073(19)	0.5783(11)	4.96(59)					
C(37)	0.16520(66)	0.8785(18)	0.6057(11)	4.50(56)					
C(38)	0.07174(60)	0.7457(17)	0.5828(10)	3.71(52)					
C(39)	0.03548(67)	0.7243(18)	0.5944(10)	4.55(57)					
C(40)	0.00127(68)	0.7457(19)	0.5488(11)	5.11(59)					
C(41)	0.00380(78)	0.7838(21)	0.4884(12)	6.72(70)					
C(42)	0.03791(65)	0.8001(17)	0.4765(10)	4.25(55)					
C(43)	0.07142(60)	0.7811(16)	0.5245(10)	3.65(51)					

species divided by the sum of the integrals for all species present. Plots of ln(mole fraction of $(\mu\text{-H})_3Ru_3(\mu_3\text{-CX})(CO)_9$) vs. time were linear for 2 to 3 half-lives, indicating a rate law which is first-order in cluster concentration, and were satisfactorily reproducible. The first-order rate constant was independent of ligand concentration over the narrow range of concentrations examined. Rate constants (Table 3) for the first and second substitutions were also determined in each kinetic experiment from the concentrations of all four cluster species, using a computer program written by Professor C.D. Ritchie (Department of Chemistry, State University of New York at Buffalo) for the solution of simultaneous first-order differential equations [13]. In general, the rate constants were taken as the average of values from duplicate runs. Estimated error limits are ±15%. Reproducibility was better than ±10%.

Kinetics of substitution on $Co_3(\mu_3\text{-CX})(CO)_9$. The rates of substitution by PPh_3 (10-fold excess) on $Co_3(\mu_3\text{-CX})(CO)_9$ (X = Cl, OMe) in heptane were determined as described by Cartner, Cunninghame and Robinson [10]. Infrared spectroscopy was used to monitor the disappearance of the starting material, as indicated by the absorbance on the highest frequency (A_1) carbonyl band. Plots of ln(absorbance) vs. time were linear for 2 to 3 half-lives. The rate was found to be independent of concentration of the ligand, as was found previously for other $Co_3(\mu_3\text{-CX})(CO)_9$ clusters. For X = OMe first-order rate constants were determined at 315.2 K (1.4×10^{-3} s^{-1}), 304.9 K (3.0×10^{-4} s^{-1}) and 297.5 K (1.0×10^{-4} s^{-1}) and activation parameters were calculated as $\Delta H^{\neq} = 26.6 \pm 0.8$ kcal/mol and $\Delta S^{\neq} = 13 \pm 2$ eu. For X = Cl only the rate constant at 315.3 K of 7.9×10^{-5} s^{-1} was determined. Both rate constants and activation parameters were calculated using a least-squares program. Error limits for the activation parameters are given as one standard deviation.

X-Ray diffraction study of $(\mu\text{-H})_3Ru_3(\mu_3\text{-CPh})(CO)_7(AsPh_3)_2$. An opaque yellow crystal of approximate dimensions 0.1 × 0.2 × 0.3 mm was placed in a thin-walled capillary tube which was then mounted in a eccentric goniometer on a Syntex $P2_1$ automated four-circle diffractometer. Alignment of the crystal and data collection were performed as previously described [14]. See Table 4 for details. The crystal was mounted such that its [10$\bar{2}$] direction was approximately coincident with the diffractometer's ϕ-axis. All data were converted to $|F_o|$ values after correction for absorption and for Lorentz and polarization factors. Reflections with $I(\text{net}) < 0$ were assigned a value of $|F_o| = 0$. It should be noted that the crystals were of rather poor quality with virtually no data observable beyond $2\theta = 35°$ (Mo-K_α radiation). The structure is thus of limited precision.

Our SUNY-Buffalo modified version of the Syntex XTL interactive crystallographic program system was used for calculations on our in-house NOVA 1200 computer. The ruthenium atoms were located by direct methods (MULTAN). The positions of the non-hydrogen atoms and hydride ligands were determined from a series of difference-Fourier calculations. The aromatic hydrogen atoms were included in idealized positions based upon sp^2 hybridization of carbon with $d(C\text{–}H) = 0.95$ Å [15]. Full-matrix least-squares refinement converged with R_F 7.2%, R_{wF} 7.2% and GOF = 3.12 for all 3208 reflections, R_F 6.0% and R_{wF} 6.0% for the 2779 reflections with $|F_o| > 3\sigma(|F_o|)$, and R_F 5.4% and R_{wF} 5.9% for the 2523 reflections with $|F_o| > 6\sigma(|F_o|)$ [16].

TABLE 6

ANISOTROPIC THERMAL PARAMETERS (B_{ij}'s, A^2) FOR $(\mu_3\text{-H})_3Ru_3(\mu_3\text{-CPh})(CO)_7(AsPh_3)_2$

Anisotropic thermal parameters (and esd) for H(3)Ru(3)CPh$(CO)_7(AsPh_3)_2$ (edsare right-justified to the least significant figure of the parameter.) The form of the anisotropic temperature factor is $T = \exp(-0.25(B_{11}h^{**2}(a^*)^{**2} + \ldots + B_{12}hka^*b^* + \ldots))$

Atom	B_{11}	B_{22}	B_{33}	B_{12}	B_{13}	B_{23}
Ru(1)	2.68(10)	2.35(10)	2.41(10)	−0.302(76)	1.381(76)	−0.033(76)
Ru(2)	2.45(11)	2.44(10)	2.59(10)	0.058(77)	1.261(79)	0.091(77)
Ru(3)	2.55(10)	2.55(10)	2.86(10)	−0.270(79)	1.186(79)	0.040(80)
As(1)	3.18(13)	2.62(12)	2.54(12)	−0.19(10)	1.53(10)	−0.005(95)
As(2)	3.11(13)	2.56(12)	3.50(13)	−0.14(10)	1.47(10)	0.24(10)
O(1A)	6.1(10)	2.37(84)	7.5(11)	1.43(75)	1.85(83)	1.10(75)
O(1B)	4.9(10)	6.8(11)	7.2(11)	−2.67(84)	3.50(85)	−2.01(84)
O(2A)	8.4(12)	5.7(10)	4.4(10)	0.09(85)	2.60(85)	−0.67(82)
O(2B)	3.54(91)	7.3(11)	7.7(11)	0.09(79)	3.55(83)	0.74(85)
O(3A)	4.10(91)	3.65(88)	9.3(12)	1.44(78)	2.71(83)	0.16(82)
O(3B)	6.5(10)	6.9(11)	6.4(10)	−1.41(87)	4.40(92)	0.98(84)
O(3C)	6.4(10)	6.3(10)	3.78(90)	−0.63(83)	0.77(78)	−1.56(83)

The analytical scattering factor [17a] for the appropriate neutral atom was corrected for both $\Delta f'$ and $\Delta f''$ components of anomalous dispersion [17b]. Least-squares refinement minimized the function $\Sigma w(|F_o| - |F_c|)^2$, where the weighting scheme is based upon counting statistics with an "ignorance factor" of 0.03. Final positional parameters are listed in Table 5 and anisotropic thermal parameters in Table 6.

Results

Group V donor ligands L (L = $AsPh_3$, $SbPh_3$, $P(OMe)_3$, PPh_3) substitute on $(\mu\text{-H})_3Ru_3(\mu_3\text{-CX})(CO)_9$ (X = OMe, Me, Cl, Ph) to yield sequentially $(\mu\text{-H})_3Ru_3(\mu_3\text{-CX})(CO)_{9-n}L_n$ ($n = 1$, 2 and 3). These substituted products can be separated by thin-layer chromatography, although in solution the mono- and di-substituted derivatives slowly disproportionate to form a mixture containing all four $H_3Ru_3(\mu_3\text{-CX})(CO)_{9-n}L_n$ species. The rates of these ligand exchanges are somewhat slower than the rates of substitution and are negligible in the presence of excess L. All products thus far isolated ($n = 1$: L = $AsPh_3$ (X = Ph); $n = 2$: L = $AsPh_3$ (X = OMe, Cl, Ph), $SbPh_3$ (X = OMe); $n = 3$: L = $AsPh_3$ (X = OMe, Me, Cl, Ph), $SbPh_3$ (X = OMe), PPh_3 (X = OMe, Ph), $P(OMe)_3$ (X = Ph)) are yellow, air-stable, crystalline complexes. These compounds have been characterized by ^1H NMR and infrared spectroscopy and in representative cases by elemental analysis. The electron-impact mass spectrum of $(\mu\text{-H})_3Ru_3(\mu_3\text{-CPh})(CO)_8(AsPh_3)$ displays a weak molecular ion and stepwise loss of eight carbonyls and the triphenylarsine ligand.

The infrared spectra (Table 1) of $(\mu\text{-H})_3Ru_3(\mu_3\text{-CX})(CO)_{9-n}L_n$ in solution display only terminal carbonyl stretches. Spectra for all complexes having the same value of n are very similar, regardless of the identity of L or X, implying similar structures. For each of the trisubstituted derivatives, axial substitution by L would give rise to a molecule having C_{3v} symmetry (structure I), while radial substitution

would most likely result in a molecule of C_3 symmetry (structure II). For the C_{3v} structure only three carbonyl stretching frequencies are expected, while four are allowed for the C_3 structure. The infrared spectrum of each species $(\mu\text{-H})_3Ru_3(\mu_3\text{-CX})(CO)_6L_3$ displays three strong bands in the terminal carbonyl region. However, in some cases very weak absorptions are also noted; these are most likely due to small amounts of disubstituted derivatives. The infrared spectra are consistent with axial substitution but cannot be used to rule out radial substitution.

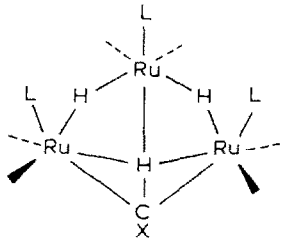

(I)

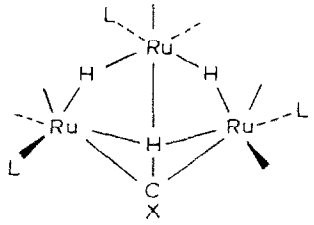

(II)

The ^1H NMR spectra (Table 2) provide the most straightforward method for characterization of the $AsPh_3$ and $SbPh_3$ derivatives. The spectra of the monosubstituted clusters each consist of a triplet, due to one hydride, which is close in chemical shift to the hydride resonance of the parent carbonyl, and a doublet (2H) which is ca. 0.5 ppm to lower field; the coupling constant between these two resonances is 3 Hz. The spectrum for each disubstituted cluster consists of a reversed pattern of a doublet (2H) close to the chemical shift of the doublet for the monosubstituted derivative and a triplet (1H) ca. 0.5 ppm to lower field; the coupling constant is again 3 Hz. The trisubstituted derivatives are characterized by singlet hydride resonances to still lower field. Thus, the spectra of the hydride region for $(\mu\text{-H})_3Ru_3(\mu_3\text{-COMe})(CO)_{9-n}(AsPh_3)_n$ in 1,2-dichloroethane are as follows: $n = 0$, τ 28.64 (s, 3 H); $n = 1$, τ 28.56 (t, 1 H), 27.94 (d, 2 H), J 3 Hz; $n = 2$, τ 27.50 (d, 2 H), 26.92 (t, 1 H), J 3 Hz; $n = 3$, τ 26.34 (s, 3 H). Apparently substitution by $AsPh_3$ or $SbPh_3$ causes downfield shifts for resonances due to hydrides bridging to the substituted metal atom. The spectra of clusters substituted with phosphorus donor ligands are more complicated because of coupling between the hydrides and ^{31}P (ca. 8 Hz) and because the downfield shifts of the hydride resonances upon substitution are somewhat smaller. The spectra of the mono- and disubstituted EPh_3 (E = As or Sb) derivatives are consistent with axial coordination by L, which would generate a plane of symmetry bisecting the metal triangle. However, a fluxional process causing intramolecular exchange of L between two radial positions on each substituted ruthenium atom would generate the same spectrum.

An osmium analog $(\mu\text{-H})_3Os_3(\mu_3\text{-CMe})(CO)_8(PEtPh_2)$ has been recently prepared by hydrogenation of $(\mu\text{-H})_2Os_3(\mu_3\text{-}\eta^2\text{-CCH}_2)(CO)_8(PEtPh_2)$ [19]. The infrared spectrum of this complex is similar to that of $(\mu\text{-H})_3Ru_3(\mu_3\text{-CPh})(CO)_8(AsPh_3)$, and its ^1H NMR spectrum contains hydride resonances at τ 28.03 (d, 2 H, J(P–H) 11.8 Hz) and 28.76 (s, 1 H); no coupling between the two hydrides was reported. The ^{13}C NMR spectrum, consisting of four carbonyl resonances of equal intensities, was interpreted as indicating axial coordination of $PEtPh_2$, but again rapid exchange of the phosphine between two radial sites on the substituted metal atom would also generate the observed spectrum.

Since the determination of the site of ligand substitution was essential to the comparison of the methylidyne-tricobalt and -triruthenium cluster systems, a single-crystal X-ray crystallographic study of $(\mu\text{-H})_3Ru_3(\mu_3\text{-CPh})(CO)_7(AsPh_3)_2$ was conducted.

Structure of $(\mu\text{-H})_3Ru_3(\mu_3\text{-CPh})(CO)_7(AsPh_3)_2$. Interatomic distances are collected in Table 7; bond angles appear in Table 8. The geometry of the molecule is

TABLE 7

INTERATOMIC DISTANCES (in Å) FOR $(\mu\text{-H})_3Ru_3(\mu_3\text{-CPh})(CO)_7(AsPh_3)_2$

(A) Ru–Ru and Ru–H distances			
Ru(1)–Ru(2)	2.864(2)	Ru(2)–H(1)	1.76(13)
Ru(1)–Ru(3)	2.848(3)	Ru(2)–H(2)	1.34(15)
Ru(2)–Ru(3)	2.863(3)	Ru(3)–H(2)	1.80(14)
Ru(1)–H(1)	1.81(13)	Ru(3)–H(3)	1.40(28)
Ru(1)–H(3)	1.67(29)		
(B) Distances within the μ_3-CPh fragment			
Ru(1)–C(1)	2.079(19)	Ru(3)–C(1)	2.116(20)
Ru(2)–C(1)	2.066(19)	C(1)–C(2)	1.451(27)
(C) Distances within the Ru–C–O Systems			
Ru(1)–C(1A)	1.935(25)	C(1A)–O(1A)	1.103(29)
Ru(1)–C(1B)	1.884(26)	C(1B)–O(1B)	1.166(31)
Ru(2)–C(2A)	1.828(26)	C(2A)–O(2A)	1.176(30)
Ru(2)–C(2B)	1.911(26)	C(2B)–O(2B)	1.133(31)
Ru(3)–C(3A)	1.919(24)	C(3A)–O(3A)	1.126(29)
Ru(3)–C(3B)	2.014(24)	C(3B)–O(3B)	1.091(30)
Ru(3)–C(3C)	1.908(26)	C(3C)–O(3C)	1.129(30)
(D) Distances involving the arsine ligands			
Ru(1)–As(1)	2.516(3)	As(1)–C(20)	1.903(22)
Ru(2)–As(2)	2.536(3)	As(2)–C(26)	1.954(21)
As(1)–C(8)	1.915(20)	As(2)–C(32)	2.014(23)
As(1)–C(14)	1.945(21)	As(2)–C(38)	1.913(22)
(E) C–C Distances in phenyl rings			
C(8)–C(9)	1.383(31)	C(26)–C(27)	1.408(34)
C(9)–C(10)	1.356(34)	C(27)–C(28)	1.437(37)
C(10)–C(11)	1.342(39)	C(28)–C(29)	1.353(40)
C(11)–C(12)	1.440(38)	C(29)–C(30)	1.329(38)
C(12)–C(13)	1.393(33)	C(30)–C(31)	1.384(33)
C(13)–C(8)	1.433(32)	C(31)–C(26)	1.353(31)
C(14)–C(15)	1.388(31)	C(32)–C(33)	1.378(31)
C(15)–C(16)	1.416(32)	C(33)–C(34)	1.348(35)
C(16)–C(17)	1.327(33)	C(34)–C(35)	1.383(36)
C(17)–C(18)	1.388(35)	C(35)–C(36)	1.312(36)
C(18)–C(19)	1.412(34)	C(36)–C(37)	1.387(36)
C(19)–C(14)	1.402(31)	C(37)–C(32)	1.384(32)
C(20)–C(21)	1.379(31)	C(38)–C(39)	1.465(35)
C(21)–C(22)	1.430(36)	C(39)–C(40)	1.380(35)
C(22)–C(23)	1.434(35)	C(40)–C(41)	1.491(37)
C(23)–C(24)	1.387(37)	C(41)–C(42)	1.380(39)
C(24)–C(25)	1.448(37)	C(42)–C(43)	1.383(33)
C(25)–C(20)	1.358(30)	C(43)–C(38)	1.401(31)
C(2)–C(3)	1.396(30)	C(5)–C(6)	1.350(32)
C(3)–C(4)	1.406(32)	C(6)–C(7)	1.423(32)
C(4)–C(5)	1.421(35)	C(7)–C(2)	1.444(33)

TABLE 8

SELECTED INTERATOMIC ANGLES (in Degree) FOR $(\mu\text{-H})_3Ru_3(\mu_3\text{-CPh})(CO)_7(AsPh_3)_2$

(A) Ru–Ru–Ru, Ru–C–Ru, Ru–H–Ru			
Ru(2)–Ru(1)–Ru(3)	60.15(6)	Ru(1)–H(1)–Ru(2)	107(7)
Ru(3)–Ru(2)–Ru(1)	59.64(6)	Ru(2)–H(2)–Ru(3)	131(9)
Ru(1)–Ru(3)–Ru(2)	60.21(6)	Ru(3)–H(3)–Ru(1)	137(20)
Ru(1)–C(1)–Ru(2)	87.40(74)		
Ru(1)–C(1)–Ru(2)	85.50(72)		
Ru(2)–C(1)–Ru(3)	86.39(72)		
(B) Angles within μ_3-CPh fragment			
Ru(1)–C(1)–C(2)	124.8(14)	Ru(3)–C(1)–C(2)	127.9(14)
Ru(2)–C(1)–C(2)	130.3(14)		
(C) Ru–Ru–(Ligand) angles			
Ru(2)–Ru(1)–C(1)	46.11(53)	Ru(3)–Ru(1)–C(1)	47.78(53)
Ru(2)–Ru(1)–H(1)	35.9(41)	Ru(3)–Ru(1)–H(1)	82.0(41)
Ru(2)–Ru(1)–H(3)	67.0(98)	Ru(3)–Ru(1)–H(3)	19.7(98)
Ru(2)–Ru(1)–As(1)	121.62(9)	Ru(3)–Ru(1)–As(1)	114.88(9)
Ru(2)–Ru(1)–C(1A)	144.92(70)	Ru(3)–Ru(1)–C(1A)	96.33(70)
Ru(2)–Ru(1)–C(1B)	94.84(71)	Ru(3)–Ru(1)–C(1B)	145.61(71)
Ru(1)–Ru(2)–C(1)	46.99(53)	Ru(3)–Ru(2)–C(1)	47.53(53)
Ru(1)–Ru(2)–H(1)	37.1(42)	Ru(3)–Ru(3)–H(1)	82.3(42)
Ru(1)–Ru(2)–H(2)	88.0(57)	Ru(3)–Ru(2)–H(2)	28.4(57)
Ru(1)–Ru(2)–As(2)	121.60(9)	Ru(3)–Ru(2)–As(2)	115.38(9)
Ru(1)–Ru(2)–C(2A)	140.53(79)	Ru(3)–Ru(2)–C(2A)	95.96(70)
Ru(1)–Ru(2)–C(2B)	94.81(69)	Ru(3)–Ru(2)–C(2B)	147.30(70)
Ru(1)–Ru(3)–C(1)	46.71(52)	Ru(2)–Ru(3)–C(1)	46.09(52)
Ru(1)–Ru(3)–H(2)	80.9(42)	Ru(2)–Ru(3)–H(2)	20.7(42)
Ru(1)–Ru(3)–H(3)	24(11)	Ru(2)–Ru(3)–H(3)	69(11)
Ru(1)–Ru(3)–C(3A)	95.26(71)	Ru(2)–Ru(3)–C(3A)	146.45(71)
Ru(1)–Ru(3)–C(3B)	118.09(66)	Ru(2)–Ru(3)–C(3B)	119.01(66)
Ru(1)–Ru(3)–C(3C)	143.67(77)	Ru(2)–Ru(3)–C(3C)	94.11(77)
(D) (Ligand)–Ru–(Ligand) angles			
As(1)–Ru(1)–C(1A)	91.02(70)	C(3A)–Ru(3)–C(3B)	92.02(96)
As(1)–Ru(1)–C(1B)	98.03(71)	C(3A)–Ru(3)–C(3C)	94.8(10)
C(1A)–Ru(1)–C(1B)	92.63(99)	C(3B)–Ru(3)–C(3C)	96.3(10)
As(2)–Ru(2)–C(2A)	96.24(78)		
As(2)–Ru(2)–C(2B)	94.91(69)		
C(2A)–Ru(2)–C(2B)	92.5(10)		
(E) (μ_3-C)–Ru–(Ligand) Angles			
C(1)–Ru(1)–As(1)	160.57(54)	C(1)–Ru(3)–C(3A)	100.66(88)
C(1)–Ru(1)–C(1A)	98.90(88)	C(1)–Ru(3)–C(3B)	160.68(84)
C(1)–Ru(1)–C(1B)	98.05(88)	C(1)–Ru(3)–C(3C)	97.08(93)
C(1)–Ru(2)–As(2)	161.09(54)		
C(1)–Ru(2)–C(2A)	94.04(95)		
C(1)–Ru(2)–C(2B)	100.47(87)		
(F) Ru–C–O angles			
Ru(1)–C(1A)–O(1A)	178.8(21)	Ru(3)–C(3A)–O(3A)	174.6(21)
Ru(1)–C(1B)–O(1B)	176.2(20)	Ru(3)–C(3B)–O(3B)	178.0(21)
Ru(2)–C(2A)–O(2A)	177.6(22)	Ru(3)–C(3C)–O(3C)	176.1(22)
Ru(2)–C(2B)–O(2B)	177.2(20)		

shown in Fig. 1. The molecule consists of a triangular arrangement of ruthenium atoms (Ru(1)–Ru(2) 2.864(2) Å, Ru(2)–Ru(3) 2.863(3) Å, Ru(1)–Ru(3) 2.848(3) Å capped by a triply-bridging benzylidyne moiety with Ru(1)–C(1) 2.079(19) Å,

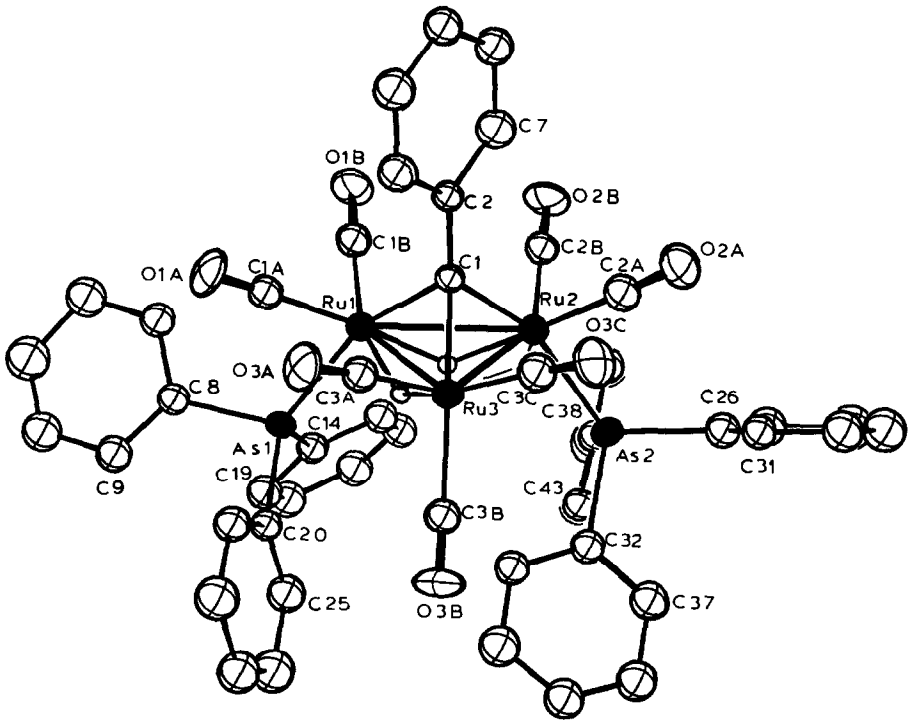

Fig. 1. Labeling of atoms in the $(\mu\text{-H})_3Ru_3(\mu_3\text{-CPh})(CO)_7(AsPh_3)_2$ molecule.

Ru(2)–C(1) 2.066(19) Å, and Ru(3)–C(1) 2.116(20) Å. (Note that the unsubstituted atom Ru(3) is associated with the longest Ru–C (alkylidyne) distance.) There are three bridging hydride ligands, each spanning two ruthenium atoms. The molecule contains six radial terminal carbonyl ligands with Ru–C distances ranging from 1.828(26) to 1.935(25) Å. The longer Ru–C distance involving the single axial carbonyl (Ru(3)–C(3B) 2.014(24) Å) illustrates the strong *trans*-lengthening effect of the μ_3-CPh ligand. All Ru–C–O angles are in the range of 176.2(20) to 178.8(21)°. Ru(1) and Ru(2) are each bonded to axial triphenylarsine ligands (Ru(1)–As(1) 2.516(3) Å, Ru(2)–As(2) 2.536(3) Å). This is consistent with spectroscopic data for the series $(\mu\text{-H})_3Ru_3(\mu_3\text{-CX})(CO)_{9-n}L_n$ in solution. An axial Group V ligand has also been reported for the related cluster $(\mu\text{-H})_2Ru_3(\mu_3\text{-PPh})(CO)_8(PPh_3)$ [20].

Kinetics of substitution on $(\mu\text{-H})_3Ru_3(\mu_3\text{-CX})(CO)_9$ by triphenylarsine. Infrared spectroscopy could not be used to monitor the progress of substitutions of $(\mu\text{-H})_3Ru_3(\mu_3\text{-CX})(CO)_9$ because extensive overlap for the spectra of the various substituted products. Because the hydride resonances for all products were well separated, ^1H NMR spectroscopy proved to be a convenient method, but presented some serious limitations upon the kinetic measurements. The low sensitivity of the technique necessitated very high concentrations of both cluster and ligand and, therefore, the range over which the ligand concentration could be varied was narrow. In addition, the trisubstituted products are much less soluble than the others and measurements could not be made after precipitation began. Finally, slow reactions required transfer of the sample between a constant temperature bath and the NMR probe, thus preventing precise temperature control. Within these constraints, results

were satisfactorily reproducible and the method was found suitable for the determination of relative rates of the first and second ligand substitutions on $(\mu\text{-H})_3Ru_3(\mu_3\text{-CX})(CO)_9$.

In the presence of a ten-fold molar excess of triphenylarsine, substitutions on $(\mu\text{-H})_3Ru_3(\mu_3\text{-CX})(CO)_9$ (X = OMe, Me, Cl, Ph) proceeded sequentially to the corresponding $(\mu\text{-H})_3Ru_3(\mu_3\text{-CX})(CO)_6(AsPh_3)_3$; no side reactions were observed. However, for X = H or CO_2Me only small amounts of substituted products were found; in these cases the predominant reaction appeared to be elimination of CH_3X and formation of $Ru_3(CO)_{10}(AsPh_3)_2$ [18]. Studies of this elimination reaction are in progress and will be reported elsewhere.

The rate law for substitution on $(\mu\text{-H})_3Ru_3(\mu_3\text{-CX})(CO)_9$ (X = OMe, Me, Cl, Ph) by triphenylarsine was found to be first-order in cluster concentration and zero-order in triphenylarsine concentration over the narrow range of concentrations examined. The rate constants k_1 (Table 3) for substitution on $(\mu\text{-H})_3Ru_3(\mu_3\text{-CX})(CO)_9$ at 298 K in 1,2-dichloroethane were found to be dependent upon the identity of X and in the relative order: X = OMe (36) $\gg$ Me (3.2) > Cl (2.3) > Ph (1); the relative rates at 308 K are slightly different but in the same order: X = OMe (62) $\gg$ Me (3.8) > Cl (2.2) > Ph (1). Our experimental results do not allow reliable determinations of activation parameters. The data for which the temperature was most closely controlled, that for X = OMe, indicate $\Delta H_1^{\neq}$ 28 kcal/mol. and $\Delta S_1^{\neq}$ 20 eu. The rate constants k_2 (Table 3) for substitution on $(\mu\text{-H})_3Ru_3(\mu_3\text{-CX})(CO)_8(AsPh_3)$ are in each case also independent of the concentration of triphenylarsine and are smaller than the corresponding value for k_1 by the statistical factor of 2/3; that is, the rate of substitution per metal atom is unaffected by the first substitution. We were unable to determine rate constants for substitution of a third ligand using NMR techniques.

Discussion

Studies of substitutions of $Co_3(\mu_3\text{-CX})(CO)_9$ have determined that the structures of the products depend upon both the ligand L and the X group [21]. The majority of the monosubstituted derivatives adopt the structure established crystallographically for $Co_3(\mu_3\text{-CMe})(CO)_8(PPh_3)$ [22], in which the phosphine is radially coordinated and only terminal carbonyls are present (structure III). However, the structures of other $Co_3(\mu_3\text{-CMe})(CO)_8L$ clusters and of di- and tri-substituted phosphine and arsine derivatives are based upon the structure established crystallographically for $Co_3(\mu_3\text{-CMe})(CO)_8(P(C_6H_{11})_3)$ [23], which has bridging carbonyls and an axially coordinated phosphine ligand (structure IV). A similar structure was found

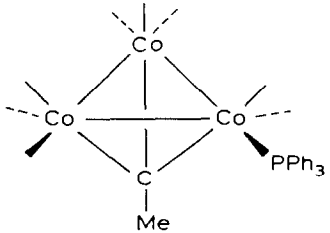

(III)

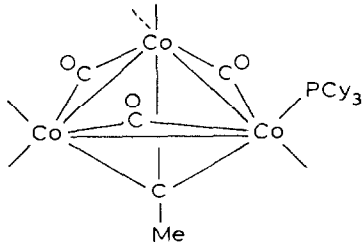

(IV)

for $Co_3(\mu_3\text{-CMe})(CO)_7$(ffars), in which the bidentate ffars ligand (ffars = 1,2-bis(dimethylarsino)tetrafluorocyclobutene) spans two cobalt atoms through the axial positions [24]. On the other hand, $Co_3(\mu_3\text{-CMe})(CO)_6(P(OMe)_3)_3$ [25] has C_3 symmetry with radially coordinated phosphite ligands. In solution, the infrared spectra of these compounds suggest the presence of both isomers.

By contrast, for $(\mu\text{-H})_3Ru_3(\mu_3\text{-CX})(CO)_{9-n}L_n$ (X = OMe, Me, Cl, Ph, L = $AsPh_3$; X = OMe, L = $SbPh_3$; n = 1, 2 or 3) only axial coordination of L with only terminal carbonyls is observed; furthermore, the propensity for di- and tri-substitution is much greater than that of the methylidynetricobalt clusters. A likely explanation for these differences is that, because of the "tilt" of the $Ru(CO)_3$ fragments, the axial positions of the methylidynetriruthenium clusters are much less crowded than the axial positions of the cobalt analogs. However, it is also possible that the hydride bridges may prevent formation of a carbonyl-bridged structure.

The rates of CO dissociation from $Co_3(\mu_3\text{-CX})(CO)_9$ are also influenced by the methylidyne substituent. Cetini, Ercoli, Gambino and Vaglio [11] found that the rate of ^{14}CO exchange decreases in the order: X = F (12) > Cl (6.5) > Br (4) > H (1) at 308–328 K. Cartner, Cunninghame and Robinson [10] found that triphenylphosphine substitution on $Co_3(\mu_3\text{-CX})(CO)_9$ to give exclusively $Co_3(\mu_3\text{-CX})(CO)_8(PPh_3)$ proceeded by a CO dissociative mechanism and that the rates decreased in the order: X = F (9.4) $\gtrsim$ Ph (8.5) > Me (2.2) > H (1) at 314 K. The results of these two studies were interpreted to indicate a decreasing Co–CO bond strength with increasing electronegativity of X; this was attributed to a lessening of the amount of π-back-bonding to the CO ligands as X becomes more electron-withdrawing. The influence of X was believed to be largely due to inductive effects.

Substitution of triphenylarsine on $(\mu\text{-H})_3Ru_3(\mu_3\text{-CX})(CO)_9$ also proceeds via a CO dissociative mechanism. This is supported by the rate law, which is first-order in cluster concentration and zero-order in ligand concentration, and by the activation parameters for substitution on the OMe derivative, which are similar to those measured for other substitutions proceeding by CO dissociation [9]. This is not surprising, since substitutions by triphenylarsine, a very poor nucleophile, are almost always of a dissociative nature. However, the relative rates found for $(\mu\text{-H})_3Ru_3(\mu_3\text{-CX})(CO)_9$ (X = OMe, Me, Cl, Ph) are not consistent with the proposal previously put forward to explain the relative rates of substitution within the methylidynetricobalt series. In particular, the OMe substituent, a good electron donor, is associated with the highest rates for substitution.

To determine whether the labilizing influence of the OMe substituent was unique to the methylidynetriruthenium cluster series, we determined the rates of substitution by triphenylphosphine on $Co_3(\mu_3\text{-CX})(CO)_9$ (X = OMe, Cl). At 315 K the rate constants were 7.9×10^{-5} s^{-1} for X = Cl and 1.4×10^{-3} for X = OMe. In combination with the data of Cartner, Cunninghame and Robinson [10], these data establish the relative rates within the $Co_3(\mu_3\text{-CX})(CO)_9$ series at 314–315 K as: X = OMe (140) $\gg$ F (9.4) $\gtrsim$ Ph (8.5) $\gtrsim$ Cl (7.9) > Me (2.2) > H (1). The OMe substituent is, therefore, a strong labilizing group for CO dissociation in both methylidyne-tricobalt and -triruthenium cluster series. There is no correlation between the degree of π-backbonding to the CO ligands and the rate of CO dissociation.

An alternative explanation for the influence of the methylidyne substituent X upon the rate of CO dissociation is based upon the π-donor properties of X, rather than upon inductive effects. A number of physical studies of the $Co_3(\mu_3\text{-CX})(CO)_9$

series have found evidence for substantial C–X π-bonding interactions. Both NQR [26] and photoelectron spectra [27–30] support delocalization of $p\pi$ levels into the Co_3C core where X = halide, OMe or NMe_2. It was suggested in one of these studies [28] that the strong π-donor interaction noted when X = OMe is of the type suggested by the valence-bond resonance structure V. The contribution from this resonance form might very likely stabilize the electron-deficient transition state for CO dissociation. The order of relative rates for other methylidyne substituents can also be explained in terms of π-donor ability, since the order of decreasing relative rates is also the order of decreasing π-donor ability (X = F > Cl > Br).

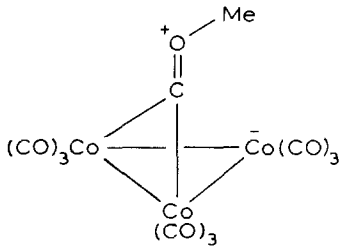

(V)

Meaningful comparisons of substituent effects within the $(\mu\text{-H})_3Ru_3(\mu_3\text{-CX})(CO)_9$ series are hampered by the drastically different steric and electronic properties of the OMe, Me, Cl and Ph substituents. A recent study of the photoelectron spectra of $(\mu\text{-H})_3Ru_3(\mu_3\text{-CX})(CO)_9$ (X = H, Cl, Br) concluded that the bonding in these clusters is similar to that in the methylidyne tricobalt analogs, although because of the differing tilts of the $M(CO)_3$ fragments in the two systems, there are some differences in the directionality of the M_3C bonds and in the nature of the HOMO's [31]. In both methylidynetrimetal series the rates of substitution are relatively insensitive to the nature of the methylidyne substituent X, unless X is a good π-donor. We should note that, although the order of relative rates for X = Me, Cl and Ph is reversed for the two cluster series, the range of rates is quite small. In this situation the relative order is likely to depend upon the temperature and without extremely accurate activation parameters, which are not now available for either methylidynetrimetal series, little can be gained from further speculation upon the origin of these substituent effects.

Conclusions

(1) Substitution on $(\mu\text{-H})_3Ru_3(\mu_3\text{-CX})(CO)_9$ (X = OMe, Me, Cl, Ph) by triphenylarsine proceeds sequentially to produce $(\mu\text{-H})_3Ru_3(\mu_3\text{-CX})(CO)_6(AsPh_3)_3$ in which the triphenylarsine ligands, one per metal atom, in all products are axially coordinated.

(2) The mechanisms of the first and second substitutions are CO dissociative with the rate constant for the second substitution statistically identical to the rate constant for the first. That is, CO dissociation at the unsubstituted metal centers is unaffected by the first substitution.

(3) The relative rates of substitution as a function of X are: X = OMe (36) $\gg$ Me

(3.2) > Cl (2.3) > Ph (1) at 298 K. The labilizing effect of the OMe substituent is attributed to stabilization of the transition state, which is electron-deficient at the site of CO dissociation, by π-donation from OMe to the Ru_3C core.

Additional data

A Table of observed and calculated structure factor amplitudes is available upon request (from M.R.C.).

Acknowledgement

This work was supported by the National Science Foundation (Grants CHE81-21059 to J.B.K. and CHE80-23448 to M.R.C.), by the Donors of The Petroleum Research Fund, administered by the American Chemical Society, and by a Conoco, Inc., Grant of Research Corporation to J.B.K. We also thank Professor C.D. Ritchie for the use of his computer for the analysis of kinetic data.

References

1 (a) D. Seyferth, Adv. Organomet. Chem., 14 (1976) 97; (b) B.R. Penfold, and B.H. Robinson, Acc. Chem. Res., 6 (1973) 73.
2 J.B. Keister, and T.L. Horling, Inorg. Chem., 19 (1980) 2304.
3 J.B. Keister, M.W. Payne, and M.J. Muscatella, Organometallics, 2 (1983) 219.
4 A.J. Carty, B.F.G. Johnson, J. Lewis, and J.R. Norton, J. Chem. Soc., Chem. Commun., (1972) 1331.
5 (a) R.B. Calvert, and J.R. Shapley, J. Amer. Chem. Soc., 99 (1977) 5225; (b) K.A. Azam and A.J. Deeming, Chem. Soc., Chem. Commun., (1977) 472.
6 M.R. Churchill, L.R. Beanan, H.J. Wasserman, C. Bueno, Z. Abdul Rahman, and J.B. Keister, Organometallics, 2 (1983) 1179.
7 L.R. Beanan, Z. Abdul Rahman, and J.B. Keister, Organometallics, 2 (1983) 2062.
8 L.M. Bavaro, P. Montangero, and J.B. Keister, J. Amer. Chem. Soc., 105 (1983) 4977.
9 D.J. Darensbourg, Adv. Organomet. Chem., 21 (1982) 113.
10 A. Cartner, R.G. Cunninghame, and B.H. Robinson, J. Organomet. Chem., 95 (1975) 49.
11 G. Cetini, R. Ercoli, O. Gambino, and G. Vaglio, Att. Accad. Sci. Torino, Cl. Sci. Fis., Mat. Natur., 99 (1965) 1123.
12 (a) C.L. Nivert, G.H. Williams, and D. Seyferth, Inorg. Synth. 20 (1980) 234; (b) D. Seyferth, J.E. Hallgren, and P.L.K. Hung, J. Organomet. Chem., 50 (1973) 265.
13 For two consecutive, first-order reactions $A \xrightarrow{k_1} B \xrightarrow{k_2} C$ the concentrations of A and B are given by: $A = A_0\, e^{-k_1 t}$ and $B = \frac{k_1 A_0}{(k_2 - k_1)} [e^{-k_1 t} - e^{-k_2 t}]$ where A_0 is the initial concentration of species A.
14 M.R. Churchill, R.A. Lashewycz, and F.J. Rotella, Inorg. Chem., 16 (1977) 265.
15 M.R. Churchill, Inorg. Chem., 12 (1973) 1213.
16 $R_F = [\Sigma/|F_o| - |F_c||/\Sigma|F_o|] \times 100\%$; $R_{wF} = [\Sigma w(|F_o| - |F_c|)^2/\Sigma w|F_o|^2]^{1/2} \times 100\%$.
17 International Tables for X-Ray Crystallography, Vol. 4, Kynoch Press, Birmingham, England, 1974, (a) p. 99–101, (b) p. 149–150.
18 M.I. Bruce, G. Shaw, and F.G.A. Stone, J. Chem. Soc., Dalton Trans, (1972) 2094.
19 S.C. Brown, and J. Evans, J. Chem. Soc., Dalton Trans., (1982) 1049.
20 M.J. Mays, and P.L. Taylor, Acta Cryst. B, 38 (1982) 2261.
21 T.W. Matheson, B.H. Robinson, and W.S. Tham, J. Chem. Soc. A (1971) 1457.
22 M.D. Brice, B.R. Penfold, W.T. Robinson, and S.R. Taylor, Inorg. Chem., 9 (1970) 362.
23 T.W. Matheson and B.R. Penfold, Acta Cryst. B, 33 (1977) 1980.
24 F.W.B. Einstein, and R.D.G. Jones, Inorg. Chem., 11 (1972) 395.
25 P.A. Dawson, B.H. Robinson, and J. Simpson, J. Chem. Soc., Dalton Trans., (1979) 1762.
26 D.C. Miller, and T.B. Brill, Inorg. Chem., 17 (1978) 240.
27 P.T. Chesky, and M.B. Hall, Inorg. Chem., 20 (1981) 4419.

28 S.F. Xiang, A.A. Bakke, H.-W. Chen, C.J. Eyermann, J.L. Hoskins, T.H. Lee, D. Seyferth, H.P. Withers, Jr. and W.L. Jolly, Organometallics, 1 (1982) 699.
29 N.C.V. Costa, D.R. Lloyd, P. Brint, W.K. Pelin and T.R. Spaulding, J. Chem. Soc., Dalton Trans., (1982) 201.
30 G. Granozzi, E. Tondello, D. Ajo, M. Casarin, S. Aime, and D. Osella, Inorg. Chem., 21 (1982) 1081.
31 D.E. Sherwood, Jr. and M.B. Hall, Organometallics, 1 (1982) 1519.